Double Sucrose-Gap Method Applied to Single Muscle Fiber of *Xenopus laevis*

SHIGEHIRO NAKAJIMA and JOSEPH BASTIAN

From the Department of Biological Sciences, Purdue University, Lafayette, Indiana 47907. Dr. Bastian's present address is the Department of Neurosciences, University of California at San Diego, La Jolla, California 92037.

ABSTRACT Passive electrical properties (internal conductance, membrane conductance, low frequency capacity, and high frequency capacity obtained from the foot of the action potential) of normal and glycerol-treated muscle of *Xenopus* were determined with the intracellular microelectrode technique. The results show that the electrical properties of *Xenopus* muscle are essentially the same as those of frog muscle. Characteristics of the action potential of *Xenopus* muscle were also similar to those of frog muscle. Twitch tension of glycerol-treated muscle fibers of *Xenopus* recovered partially when left in normal Ringer for a long time (more than 6 h). Along with the twitch recovery, the membrane capacity increased. Single isolated muscle fibers of *Xenopus* were subjected to the double sucrose-gap technique. Action potentials under the sucrose gap were not very different from those obtained with the intracellular electrode, except for the sucrose-gap hyperpolarization and a slight tendency toward prolongation of the shape of action potential. Twitch contraction of the artificial node was recorded as a change of force from one end of the fiber under the sucrose gap. From the time-course of the recorded force and the sinusoidal stress-strain relationship at varying frequencies of the resting muscle fiber, the time-course of isotonic shortening of the node was recovered by using Fourier analysis. It was revealed that the recorded twitch force can approximately be regarded as isotonic shortening of the node.

INTRODUCTION

Application of the double sucrose-gap technique (Julian et al., 1962; Stämpfli, 1963) to single muscle fibers of the frog is very difficult. Although Stämpfli (1963) and Ildefonse and Rougier (1972) have accomplished this, our attempt was a failure. We found that the action potential of isolated muscle fibers of the frog tended to be prolonged or the membrane easily lost excitability when we used the sucrose-gap technique of the Julian et al. type. This might have arisen from the species difference of frog, or it could be due to the

fact that we did not apply Vaseline seals at the interface between sucrose and Ringer solutions.

After having spent some time, we switched to the African clawed toad (*Xenopus laevis*), and found that muscle from *Xenopus* was more amenable to sucrose-gap experimentation. An additional advantage of using *Xenopus* is that the animals stay healthy indefinitely in the laboratory, allowing us to obtain good material regardless of the length of captivity.

One of the aims of the present investigation is to describe the electrical properties of the skeletal muscle fiber of *Xenopus* in comparison with those of frog. The other purpose is to examine various technical problems attached to the sucrose-gap method when applied to isolated single muscle fibers of *Xenopus*.

METHODS

Twitch muscle fibers from m. sartorius, m. iliofibularis, and m. flexor brevis digiti V of *Xenopus laevis* were used. In a few experiments the sartorius muscle of frogs (*Rana pipiens*) was also used. *Xenopus* were fed on beef heart and vitamins. They stayed in good health indefinitely.

Microelectrode

The microelectrode technique was the conventional one. Current-passing electrodes were filled with 2 M K citrate and potential electrodes with 3 M KCl. The constant current condition was maintained by a feeeback circuit (Fig. 2); the circuit characteristics will be described below. Experiments with the microelectrode were done on muscles stretched to 115% of the slack length.

Sucrose Gap

Single fibers were isolated from m. flexor brevis digiti V. of *Xenopus*. This particular muscle was chosen because of the presence of tendons of a reasonable length on both ends. The length of the fiber was about 6 mm, and was convenient for our sucrose-gap apparatus. With a longer muscle, such as the iliofibularis, recording of twitch force would have been difficult (see page 251).

The method of double sucrose gap was very similar to that used for giant axons in Drs. J. W. Moore and T. Narahashi's laboratories. We owe our success to their advice, and they should be credited for most of the technical details described here. In principle the method is identical to the one described in Julian et al. (1962), but in practice it is different. An isolated fiber was laid in a small trough (Fig. 1) about 400 μm in width and about 2.7 mm in length. Each tendon was tied with fine enamel-coated silver wires to a hook fashioned from glass tubing, one of which was connected to a piezo-resistive strain gauge (Pixie 8206, Endevco Div. Becton, Dickinson & Co., Pasadena, Calif.) The characteristics were described by Chapman (1970). The fiber was stretched to about 130% of the slack length, and was positioned at about the center of the trough so that it would not touch the wall of the trough during contraction. The trough was covered by a Mylar (E. I. Dupont de

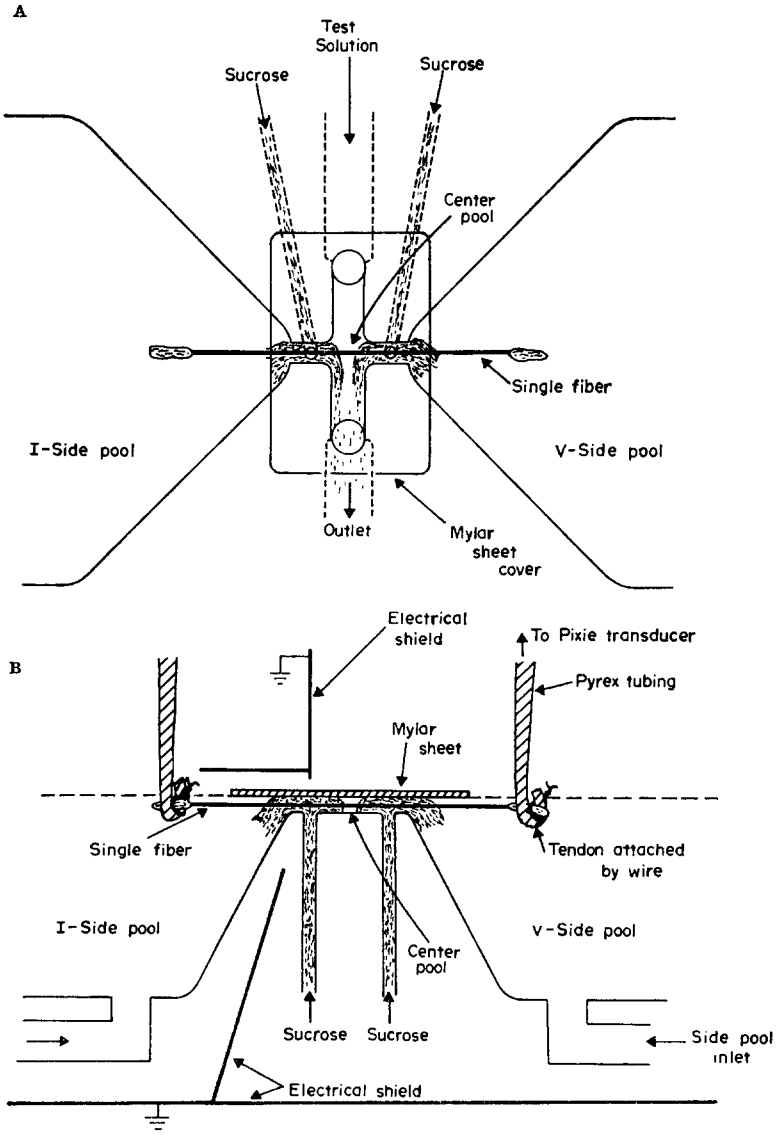

FIGURE 1. Top view (A) and side view (B) of the sucrose-gap apparatus. The figure is roughly to scale. The size of Mylar sheet cover is 4 × 6 mm. Further details in text.

Nemours & Co., Wilmington, Del.) sheet resulting in a water-tight tunnel, and the flows of the Ringer solution into the three pools (I-side pool, V-side pool, and center pool) were started. This was followed by a flow of isotonic sucrose solution, which entered the tunnel through two holes about 400 μm in diameter, and flowed into the center pool and the two side pools, thus making sharp border lines between the sucrose and the Ringer solutions. The border lines were clearly visible under the stereomicroscope. We did not apply Vaseline seals at the interface between sucrose and the

Ringer solution. The length of the node was adjusted by changing the flow rate of the center pool. The inflow rate of each solution was controlled by a needle valve. The outlet of the center pool was a vinyl tube with cotton inside, and the solution leaked out from the tapered tip of the cotton forming fine drops. The level of the solution in the V-side pool and I-side pool was maintained by suction through a glass capillary into a negatively pressurized bottle. The inside of these suction tubes was coated with an antiwetting agent.

In Fig. 2, the equivalent circuit of the sucrose gap and the voltage- and current-clamping system is shown. Z is the transfer impedance of the artificial node. R_v and R_c represent the internal resistance of the fiber between the V-side pool and the center pool, and that betwen the I-side pool and the center pool, respectively. Z_e is the input impedance of the fiber segment lying inside the side pool. The value of R_v (or R_c) plus R_e (the parallel resistive element of Z_e) in series was measured by applying a small low frequency sinusoidal current (10 Hz) between the side pool and the center pool, with the fiber placed in the trough and the sucrose flowing. The impedance between the two pools, minus the transfer impedance of the nodal membrane gave the value of $(R_v + R_e)$. Since the sucrose column produces some short circuit, the obtained value of $(R_v + R_e)$ may be an underestimate by a few percent. The value of $(R_v + R_e)$ was about 0.7 MΩ in a fiber of 100 μm in diameter just after the completion of the impedance experiments (i.e., about 30 min after the start of the sucrose flow). The value would have varied as the time passed, but no systematic study was conducted to assess this point.

R_{sv} and R_{sc} are the longitudinal resistances of the sucrose columns. These were estimated simply by measuring the resistance between the two pools by applying 10 Hz sinusoidal current, while the sucrose was flowing, but without the fiber lying in the trough. The value was between 20 and 30 MΩ. Since during the real experiments the muscle fiber occupied some space inside the sucrose columns, the obtained values of R_{sv} and R_{sc} would have been an underestimate by about 5%.

Muscle fibers have a larger value of membrane capacity and a larger value of internal resistance than the squid or the lobster axons. Both of those properties set unfavorable conditions for a stable and fast-responding voltage clamping. Thus, the stray capacities around the system had to be made as small as possible. Analogous to the case of the two microelectrode experiments (Falk and Fatt, 1964), there are four different stray capacities that would affect electrical recording. In Fig. 2, C_1 is the capacity of the input circuit to the ground. In order to reduce this capacity, electrical continuity of the V-side pool to the reservoir of the solution was disconnected by inserting a buffer stage through which the solution passed by dripping. The capillary tubing used for suctioning the fluid in the V-side pool was covered by a shield which was connected to the output of the cathode follower stage. The value of C_1 was measured, with the sucrose flowing but without the fiber set in the trough, by sending square-wave voltage through a 4.7-MΩ resistor into the V-side pool. The transient response of the voltage change of the V-side pool would be determined by $(C_1 + C_2)$ and the equivalent resistance between the V-side pool and the ground. Because of a small stray capacity (about 0.3 pF) in parallel with the 4.7-MΩ resistor, the procedure may produce an underestimate of the real value of C_1. C_1 was usually adjusted to about 2 pF with the capacity neutralized through the input stage before experiments.

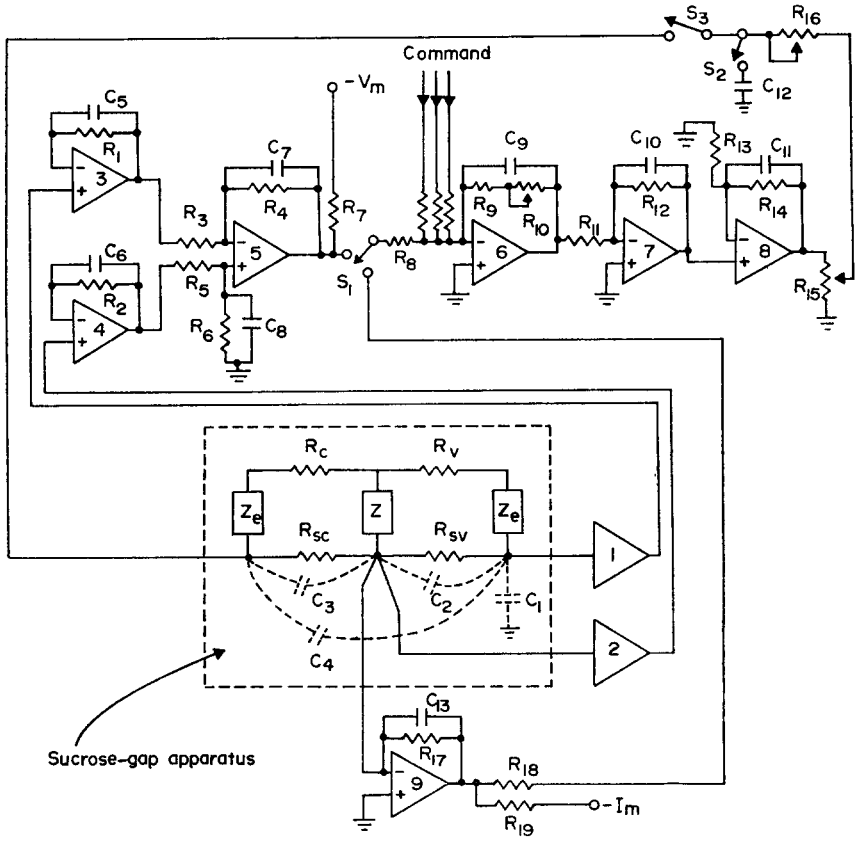

FIGURE 2. Voltage- or current-clamping circuit with an equivalent circuit of the sucrose-gap apparatus. Z = transfer impedance of the artificial node. Z_e = input impedance of the part of the fiber inside the left and right side pools. R_v and R_c = internal resistances of the part of the fiber inside the sucrose solution. R_{sv} and R_{sc} = longitudinal resistances of the sucrose columns surrounding the fiber. C_1, C_2, C_3, C_4 = stray capacitances that introduce errors in electrical measurement. Amplifiers: 1 and 2 = negative capacity amplifier (gain 1). 3, 4, 5 = Philbrick P-25 or P-85. 6 = Philbrick 1011. 7 = Philbrick P-45. 8 = Philbrick power operational amplifier 1022. 9 = Philbrick 1011; I-V converter Teledyne-Philbrick, Dedham, Mass. R_1, R_2 = 1 kΩ. R_3, R_4, R_5, R_6 = 2 kΩ. R_7 = 10–100 Ω inserted to prevent a capacitative load of a long wire. R_8, R_9 = 1 kΩ. R_{10} = 10 kΩ (when used for microelectrode expriments, about 30 kΩ), R_{11} = 1 kΩ. R_{12} = 4.7 kΩ. R_{13} = 10 kΩ. R_{14} = 150 kΩ. R_{15} = 50 kΩ. R_{16} = 20 MΩ. R_{17} = 100 kΩ or 1 MΩ. R_{18}, R_{19} = 470 Ω to prevent capacitative loads of long wires. C_5, C_6 = 50 pF. C_7, C_8 = 320 pF. C_9 = 1.2 pF. C_{10} = 58 pF. C_{11} = 4.7 pF. C_{12} = 0.1–0.5 μF used only for current clamping. C_{13} = 2.5–25 pF.

C_2 is the capacity between the V-side pool and the center pool, and C_3 is the one between the I-side pool and the center pool. C_4 is the capacity between the two side pools. These capacities were minimized by constructing the three pools in proper shape (Fig. 1): both side pools apposing the center pool with minimum areas. A grounded shield

was inserted from beneath deep into the space between the I-side pool and the center pool. Other shields covered the apparatus from above and below (Fig. 1 B). These stray capacities were measured by applying sinusoidal current (10–2,000 Hz) between the V-side and the center pool and between the I-side and the center pool, while the sucrose was flowing but without the fiber in the trough. By analyzing the transfer impedances (between the V-side and the center, between the I-side and the center, and between the V-side and the I-side pool), obtained from Lissajous figures, C_2, C_3, and C_4 were calculated. The method is essentially the same as that described in detail by Falk and Fatt (1964). Usually C_2 was about 1 pF, C_3 0.3 pF, and C_4 0.03 pF.

The voltage- and current-clamping circuit illustrated in Fig. 2 has a maximum overall voltage gain of about 800 and a frequency response of about 30 kHz at 3 dB down. When used for the microelectrode study the gain was increased to about 2,500. The amplifier 8, the power operational amplifier, can deliver a voltage of ± 100 V. Frequency response of the voltage recording system, namely, the system comprising amplifiers 1, 2, 3, 4, 5, and oscilloscope, was, without input resistance attached, about 150 kHz at 3 dB down, with a common mode rejection of 1:800 at 10 kHz and 1:300 at 50 kHz. The frequency response of the current recording system was usually 70 kHz at 3 dB down. C_{12} was the frequency-limiting element, used only under the current-clamping condition. Under the voltage-clamping condition, the nodal membrane (Z) itself becomes the frequency-limiting element, and thus an additional frequency-limiting element of a comparable time constant produces instability. In order to achieve a stable voltage-clamping, the phase-shift of the transfer impedance of the node (Z) should be as small as possible. A long nodal length would result in a larger phase shift. Thus, the nodal length should be as short as possible. But too short a nodal length deteriorated the fiber quickly. Experiments were conducted with the nodal length varying from 50 to 500 μm according to the aim of the particular experiment.

The potential electrodes were Ag-AgCl electrodes. The current electrode in the center pool was a fine platinum-black wire (100 μm in diameter), and was placed very close to the membrane of the artificial node in order to make the series resistance between the membrane and virtual ground (the input to amplifier 9 of Fig. 2) negligible.

The normal Ringer solution had the following composition; Na^+ 120; Cl^- 121; K^+ 2.5; Ca^{++} 1.8; HPO_4^{--} 2.15; $H_2PO_4^-$ 0.85 mg ion/liter. The sucrose solution had a concentration of 214 mM with a specific conductivity of about 10^{-6} mho/cm.

RESULTS

Microelectrode Study

PASSIVE ELECTRICAL PROPERTIES The internal conductivity (G_i), membrane conductance (G_M), and membrane capacity (C_M) were measured in the same way as in Hodgkin and Nakajima (1972 *a*). Single fibers were isolated from the sartorius muscle of *Rana pipiens*, and the iliofibularis muscle of *Xenopus*. Diameters (D) of the fiber were measured at seven points along the fiber with a stereomicroscope at $\times$ 200 magnification from two directions at an angle of about 90° with each other. Two microelectrodes (resistance about 10 MΩ, sharpness of the tip being checked under the microscope before use) were

inserted into a fiber. Small rectangular current pulses were passed through the current electrode, and the potential changes were recorded at several locations (three to five locations in the case of frog muscle experiments and 6–10 locations in *Xenopus* experiments) at distances varying between 100 μm and 2 mm. At each location two records of anodal and two records of cathodal potentials were photographed. From these data, the values of G_i, G_M, and C_M were calculated by the cable theory. The results are summarized in Table I. Although the number of fibers is not large, the data suggest that the passive electrical properties of *Xenopus* muscle are essentially the same as those of frog muscle.

TABLE I

MEMBRANE CONSTANTS OF SINGLE ISOLATED FIBERS

	D	Resting potential	G_i	G_M	C_M low frequency	Number of fibers
	(μm)	(mV)	($mmho/cm$)	($mmho/cm^2$)	($\mu F/cm^2$)	
Rana pipiens, sartorius	84±6.7	−86.8±2.5	6.78±0.85	0.356±0.039	6.6±0.59	8
Xenopus laevis, iliofibularis	89±8.5	−88.0±1.9	5.82±0.28	0.485±0.064	6.6±0.48	5

The values are Mean ± SEM. Experiments were performed at a bath temperature between 23.0 and 25.0°C., and the values of G_i and G_M were corrected to 20.0°C using the temperature coefficients in Hodgkin and Nakajima (1972 *a*).

GLYCEROL-TREATED FIBERS OF *XENOPUS* Whole sartorius muscles or bundles of a few fibers from the iliofibularis muscle were used. They were detubulated by the standard procedure (Howell and Jenden, 1967; Gage and Eisenberg, 1969); i.e., immersion in a Ringer solution containing 400 mM glycerol for 1 h, and then returning to normal Ringer. The fibers were used for experimentation after allowing more than 1 h for equilibration in normal Ringer. When using the whole sartorius muscle, the thin connective tissue layer covering the inner surface of the muscle was dissected away, a procedure which facilitated an easy and secure insertion of electrodes.

The method of obtaining the value of capacity from the foot of action potential was the same as in Hodgkin and Nakajima (1972 *b*). First two microelectrodes were inserted and the cable analysis by square-wave current pulses was conducted as described above. Then three microelectrodes, one for current and two for voltage, were inserted in order to obtain the shape and velocity of the action potential.

In Table II A and B, the results are summarized. The capacity C_f was calculated by the equation:

$$C_f = \frac{DG_i}{4\theta^2\tau_f} - \tau_f G_M, \qquad (1)$$

TABLE II

MEMBRANE CAPACITY OF *XENOPUS* GLYCEROL-TREATED FIBER FROM THE FOOT OF ACTION POTENTIAL (C_f)

	D	Height of A.P.	θ	τ_f	G_M	C_f	C_M low frequency	Number of fibers
	μm	(mV)	(m/s)	(μs)	$(mmho/cm^2)$	$(\mu F/cm^2)$	$(\mu F/cm^2)$	
(A) Sartorius 1–2 h after glycerol treatment	91±3.8	126±2.2	3.67±0.15	107±2.4	0.490±0.042	0.96±0.05	1.28±0.06	10
(B) Iliofibularis, 1–2 h after glycerol treatment	107±5.5	126±2.5	4.03±0.21	98.8±4.1	0.388±0.03	1.06±0.06 (0.67~1.35)	1.39±0.08 (0.99~1.91)	13
(C) Iliofibularis, 24 h after glycerol treatment	109±6.2	133±2.8	3.18±0.14	105±4.1	0.305±0.02	1.60±0.06 (1.34~1.87)	3.19±0.29 (2.35~4.55)	9

The values are Mean ± SEM. Temperature, 21.0–23.0°C. $C_f = DG_i/4\,\theta^2\tau_f - \tau_f G_m$. C_M (low frequency) was measured by cable analysis using rectangular pulses. Only the fibers with action potential height more than 114 mV were sampled. Some fibers in A showed very small twitch after the glycerol treatment. We did not include the data from those fibers. Diameter was estimated from the standard value of G_i. Group C consisted of different fibers from group B. The values in paretheses are ranges.

in which D is diameter, θ is conduction velocity, τ_f is the time constant of foot of action potential. The values obtained for C_f (0.96 or 1.06 μF/cm^2) are in fair agreement with the value for the glycerol-treated muscle of *Rana temporaria* (0.90 μF/cm^2, Hodgkin and Nakajima, 1972 *b*). However, the low frequency capacity (C_M) of *Xenopus* measured by the pulse method seems to be somewhat smaller than that of *Rana temporaria* (1.28 or 1.39 μF/cm^2 in *Xenopus*; 1.87 μF/cm^2 in frog).

It has been reported that some of the effects of the glycerol treatment such as disappearance of twitch or the inaccessibility of ferritin to the T system were restored when the fiber was returned to the glycerol-added Ringer (Krolenko, 1969; Zachar et al., 1972). Partial restoration was also reported when the muscle was left in normal Ringer, provided that the glycerol treatment was mild (110–220 mM glycerol, Krolenko and Fedorov, 1972).

In *Xenopus* muscle, we observed that the effects of the standard glycerol treatment (400 mM glycerol, 1 h) were partially reversible when the muscle was left in normal Ringer for a long time. Fig. 3 shows an example. In this experiment a bundle consisting of three fibers was used. Isometric twitch tensions were periodically recorded. Upon replacement of normal Ringer by 400 mM glycerol Ringer, the twitch tension was reduced drastically followed by a gradual recovery over 1 h. The fibers were then returned to normal Ringer resulting in a complete disappearance of tension. But about 6 h after the completion of glycerol treatment, the twitch began to reappear and gradually increased over the next 20–30 h. At the end of the experiment all three fibers appeared healthy under the microscope.

Five experiments of this kind were performed. Stimulus frequency varied from experiment to experiment, usually once every 27 min, never exceeding once every 10 min. Fibers were never tetanized. All five bundles showed a complete disappearance of twitch, and produced a subsequent recovery of twitch tension, the tension at 24 h being on the average 13.4% of the control ranging from 6.0 to 25.2%. These five bundles consisted of totally 19 fibers, and 7 fibers out of the 19 had completely deteriorated and disappeared within 24 h. Thus for the fibers that survived, the recovery would have been approximately 20% of the control.

Along with the recovery of twitch, membrane capacity also increased. Comparison of B and C of Table II indicates that C_f and C_M became substantially larger at 24 h after the glycerol treatment compared with the values at 1–2 h. One problem when comparing B and C is that there is a possibility that only the fibers that had had a relatively large capacity after the glycerol treatment might have survived 24 h, and the difference in capacity may not represent the true situation. It would be impossible[1] to assess how much error

[1] A rough idea of the extent of the error can be estimated. Assume that only the fibers with a large capacity survived, and that the survival rate at 24 h was $1\frac{3}{19}$. Then, 8 fibers with the largest capacity

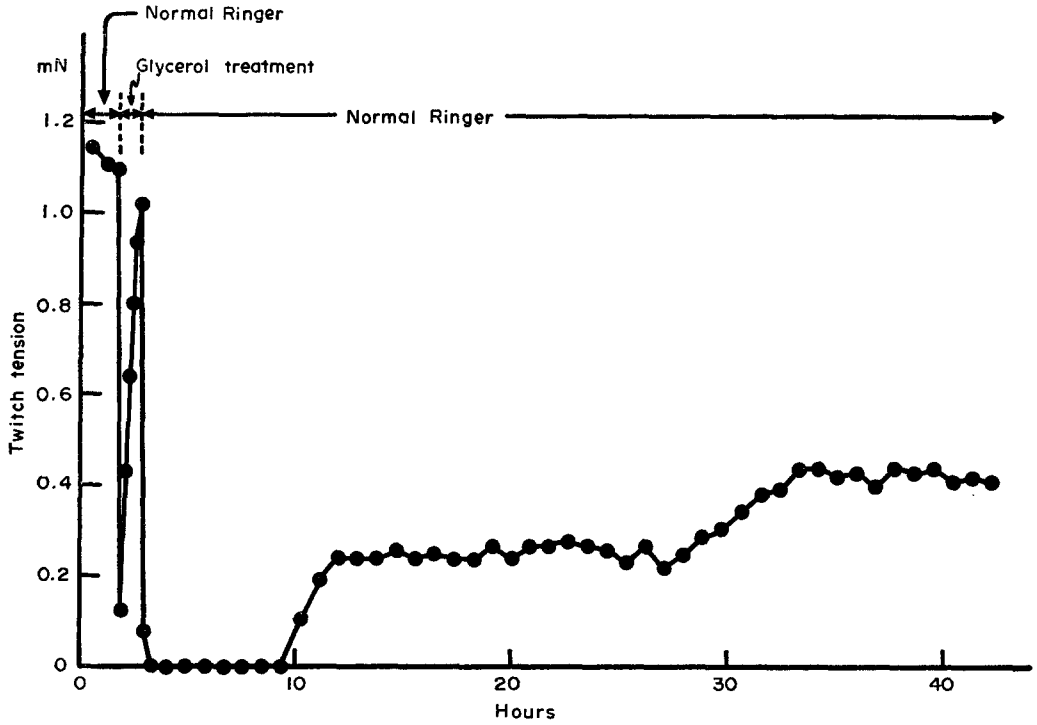

FIGURE 3. Spontaneous recovery from the "glycerol treatment." A muscle bundle consisting of three fibers from m. iliofibularis of *Xenopus* was used. The ordinate is the twitch height of the bundle under isometric condition. The external solution was changed from normal Ringer to a Ringer solution containing 400 mM glycerol (glycerol treatment). After 1 h, the solution was changed back to normal Ringer. The twitch disappeared quickly, but it started to reappear after 6 h in the normal Ringer solution. At the end of the experiment all three fibers appeared healthy under the microscope. Temperature 20–21°C.

could be produced by this effect. But it becomes obvious that a recovery of capacity did take place when we compare the "ranges" of the capacity values, which are shown in parentheses in Table II, B and C.

The above results of partial recovery of twitch and capacity suggest that the principal effect of glycerol treatment is probably not a morphologically obvious destruction of the T system, since it is somewhat unlikely that the destruction can be recovered during this period of time. It has been suggested (Krolenko and Fedorov, 1972; Nakajima et al., 1973) that the narrowing or obliteration of the T system to surface openings could be the main mechanism of the glycerol treatment. The present results could be interpreted as indicat-

out of 13 fibers of group B would correspond to the fibers that survived. The values of C_f of these 8 fibers was 1.19 ± 0.041 (Mean ± SEM), and C_M was 1.59 ± 0.065. Both values are significantly smaller ($P < 0.01$) than the values in the 24-h group.

ing that these narrowings are partially reversed when the fiber is left in normal Ringer for a long time.

Sucrose-Gap

SUCROSE-GAP HYPERPOLARIZATION In Fig. 4 time-courses of changes in the resting potential and the peak of action potential after starting the flow of the solutions are illustrated. The ordinate is the potential of the V-side pool in reference to the potential of the center pool. The records were taken once

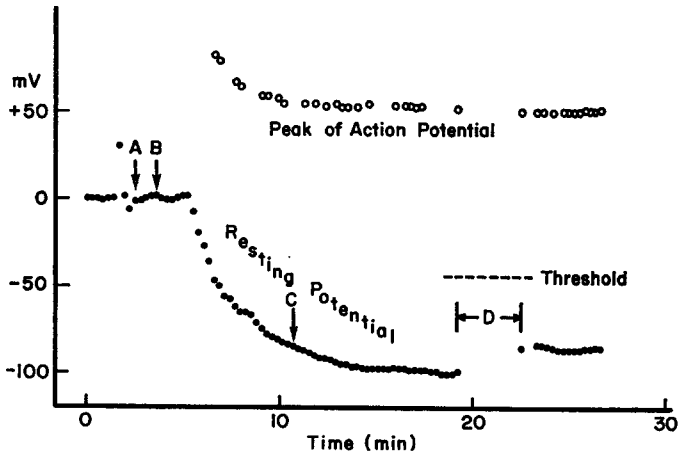

FIGURE 4. Changes in resting and action potentials of a *Xenopus* muscle fiber during the "stabilizing period" to prepare for further experiments. The ordinate is the potential of the V-side pool minus the potential of the center pool. At about the zero time flows of the solutions were started. At A a stable "artificial node" of 360 μm length wat established. At B the Ringer solution flowing into the V-side pool was switched to an isotonic KCl Ringer. At C, depolarization of the membrane in the V-side pool was probably completed. During D, the threshold for action potential was measured. Fiber diameter 97 μm. Temperature 24.0°C.

every 16.4 s. At about the zero time, flows of the solutions were started, and at the point A a stable "artificial node" of 360-μm length was established. At B the solution flowing into the V-side pool was switched from the normal Ringer into an isotonic KCl Ringer. Following a latency, which was due to a dead space, the potential of the V-side pool began to decline indicating a depolarization of the membrane in the V-side pool. At about the time indicated by C, the potassium depolarization seemed to be completed, and the subsequent shift of the potential toward the negative direction probably represented the sucrose-gap hyperpolarization (Julian et al., 1962; Stämpfli, 1963; Blaustein and Goldman, 1966), because the peak level of the action potential stayed almost constant from C and thereafter. During the period marked D, we measured the threshold of action potential (the broken line).

Subsequently, the hyperpolarization of the node was bucked up to a level which required a critical depolarization of about 40 mV by unbalancing the current-clamping circuit. All the experiments described in this and the subsequent papers were performed after this "stabilizing period." Since the absolute membrane potential is not important for our present purposes, many of the experiments have also been done without depolarizing the membrane of the V-side pool by KCl Ringer. Many of the experiments were also performed without bucking up the hyperpolarization, depending on the purpose of the experiment.

ACTION POTENTIAL The action potential of *Xenopus* muscle is similar to that of frog muscle. Fig. 5 A shows a conducted action potential recorded with microelectrode, and B shows an action potential locally stimulated by a current electrode inserted close to the potential electrode. Table III, rows A1 and A2 summarize characteristics of action potential of *Xenopus* muscle re-

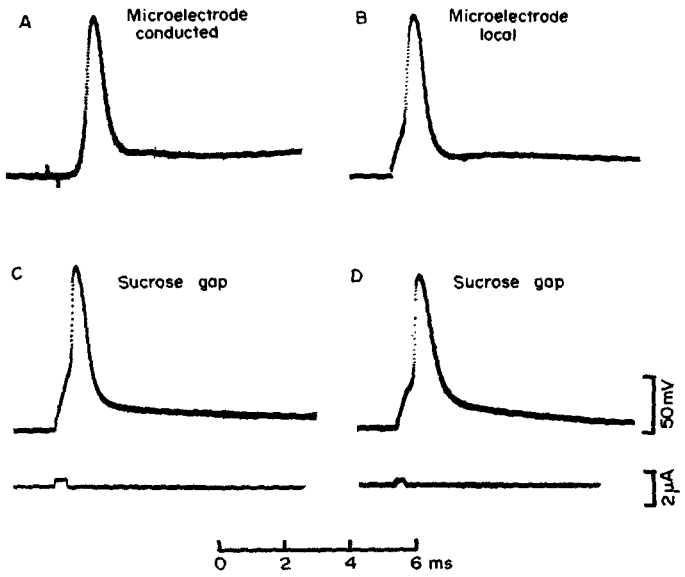

FIGURE 5. Action potentials of *Xenopus* muscle (m. flexor brevis digiti V) recorded with the intracellular microelectrode and with the sucrose gap. (A) Recorded with microelectrode. The intracellular stimulating electrode was located away from the potential electrode. Resting potential was −93 mV. (B) Recorded with microelectrode. The intracellular stimulating electrode was located 170 μm from the potential electrode. Resting potential was −89 mV. (C) Sucrose gap. Fiber diameter 186 μm. Nodal length 276 μm. Buck-up voltage 15 mV. (D) Sucrose gap. Fiber diameter 84 μm. Nodal length 338 μm. Buck-up voltage 12 mV. In C and D recording was made by a four-beam oscilloscope, two other beams being used to record twitch and action potential on a slower time base. The latter beams were erased, and the crossover points of the beams were retouched. In both C and D the current intensities were very near the threshold values. Temperature 23–24°C.

TABLE III

CHARACTERISTICS OF ACTION POTENTIAL OF NORMAL MUSCLE OF *XENOPUS* AND *RANA TEMPORARIA*

	Resting Potential (*mV*)	Action potential height (*mV*)	Duration* of action potential (*ms*)	$\dot{V}_{max}$ (*V/s*)	$-\dot{V}_{min}$ (*V/s*)	Critical depolarization (*mV*)	Number of fibers
(A) Microelectrode							
(1) *Xenopus*, sartorius	−86±1.0	129±1.1	0.79±0.02	640±23	190±6		35
(2) *Xenopus*, flexor brevis digiti V	−91±0.8	137±0.7	0.73±0.02	750±18	220±6	42‡±1.8	21
(3) § *R. temporaria*, semitendinosus and sartorius	−88	124	0.92	495	158		20
(B) Sucrose gap							
Xenopus, flexor brevis digiti V		155±1.9	0.74±0.02	1300±22	180±6	58‖±1.8	46

The values are Mean ± SEM. Temperature was 22.5–24.5°C in *Xenopus* experiments and 19.5–22.5°C in *Rana temporaria* experiments. The data of sucrose-gap experiments were obtained from May 1971 to March 1972. During this period 71 fibers were subjected to experiments in the normal Ringer at room temperature under the sucrose gap. Of these, 14 fibers were inexcitable, or produced only small action potentials which deteriorated quickly. 11 fibers showed prolonged action potentials of more than 1.1 ms in duration. These 25 experiments were thought to be failures, and were not included in any data in this series of papers. $\dot{V}_{max}$ is the maximum rate of rise. $-\dot{V}_{min}$ is the maximum rate of fall.

* Duration of action potential was measured at −30 mV in the microelectrode experiments, and at 76 mV from the peak of action potential in the sucrose-gap experiments (76 mV from the peak would correspond to −30 mV membrane potential).

‡ Quoted in Adrian et al. (1970).

§ n = 6 instead of 21.

‖ n = 24 instead of 46.

corded with microelectrodes. The frog muscle data (*Rana temporaria*) are also included for comparison (A3). The action potential of *Xenobus* appears to have a faster rate of rise and a shorter duration than that of frog. But these differences disappear when the small difference in experimental temperature is taken into account (for the temperature dependence of these quantities see Table 8 of Adrian et al., 1970).

Fig. 5 C and D shows examples of *Xenopus* action potential recorded with the sucrose-gap method, the sucrose-gap hyperpolarization being bucked up. Table III B summarizes the data. All the data were from action potential before bucking up the sucrose-gap hyperpolarization. The average height of action potential was 155 mV, which is higher than the action potential recorded by microelectrode (137 mV in the flexor brevis). This difference is probably accounted for by the sucrose-gap hyperpolarization, since there is roughly the same difference in the values of critical depolarization for the initiation of action potential (58 vs. 42 mV).

The maximum rate of rise ($\dot{V}_{max}$) obtained with the sucrose-gap group (1,300 V/s) is greater than that with the microelectrode (750 V/s). This cannot be attributable to an effect of the higher resting potential, since application of about 20-mV depolarization did not considerably alter the value of

the rate of rise. It would be due in part to the shorter time constant (about 3 μs) of the sucrose-gap system than that of the microelectrode system. Sometimes the action potential showed a prolonged configuration under the sucrose gap. Sucrose probably had some deleterious effect on the potassium permeability mechanism. We did not include fibers with prolonged action potentials in Table III B, and all the data of the sucrose-gap method at room temperature presented in this series of papers (except for the experiments of measuring membrane capacity) were derived from this sample of 46 fibers listed in Table III B (see the legend of Table III for the procedure of sampling).

Since the resistance of the sucrose solution is not infinite, the recordable potential is not exactly the same as the potential of the node. When an action potential occurs, the nodal impedance (Z in Fig. 2) becomes very small compared with the sucrose resistance R_{sv} and R_{sc}. Therefore, the short-circuiting factor is approximately given by $R_{sv}/(R_{sv} + R_v)$ (Julian et al., 1962; Stämpfli, 1963), and was about 0.98 in the present case (Z_e becomes negligible at high frequency). In summary, although a rapid loss of excitability or prolongation of the action potential occurred in some fibers with the sucrose gap, the sample of fibers used in this series of papers for a long time gave action potentials quite similar to those recorded with intracellular microelectrode.

MEMBRANE CAPACITY BY SUCROSE-GAP Membrane capacity was measured by the sucrose-gap method. A single muscle fiber of *Xenopus* was set in the sucrose-gap apparatus. Under current-clamping condition subthreshold sinusoidal currents, ranging from 1 Hz to 2 kHz, were injected, and the current-voltage Lissajous figures were photographed. Immediately after each experiment, $(R_v + R_e)$, $(R_c + R_e)$, R_{sv}, R_{sc}, and the four stray capacities (Fig. 2) were measured. In a typical experiment (Fiber X-121, Table IV) these values were: $(R_v + R_e) = 0.4\ \text{M}\Omega$; $(R_c + R_e) = 0.4\ \text{M}\Omega$, $R_{sv} = 24\ \text{M}\Omega$,

TABLE IV

MEMBRANE CAPACITY OF NORMAL MUSCLE FIBER OF *XENOPUS* BY SUCROSE GAP

Fiber reference	D	Nodal length	C_M at 1010 Hz	C_M at 2010 Hz
	μm	μm	($\mu F/cm^2$)	($\mu F/cm^2$)
X-19	84	215	4.17	3.79
X-117	127	243	3.11	2.56
X-118	165	117	2.88	2.20
X-119	162	193	1.63	1.40
X-120	160	154	2.34	1.90
X-121	147	154	3.00	2.06
Mean ± SEM	141	179	2.86±0.35	2.32±0.33

The sucrose-gap hyperpolarization was not bucked up. The temperature was from 22.5 to 24.0°C.

R_{sc} = 20 MΩ, C_1 = 2.5 pF, C_2 = 1.3 pF, C_3 = 0.32 pF, C_4 = 0.04 pF. The Lissajous records were analyzed, and the observed value of transfer impedance, Z_{ob} = (change of V_m)/(change of I_m), see Fig. 2, was obtained. From these data the real value of transfer impedance Z (Fig. 2) had to be computed by correcting for the errors due to capacitative and conductive leaks. The problem is to obtain the relationship between the transfer impedance Z and the observed impedance Z_{ob}. The solution is:

$$Z = \frac{A - Z_{ob}(C + D + EA + FA)}{Z_{ob}(BF + DE) - (AF + D)}, \tag{2}$$

in which: $A = Y_4$, $B = Y_1Y_3 + Y_2Y_3 + Y_2Y_4 + Y_3Y_4$, $C = Y_1Y_3 + Y_2Y_3 + Y_1Y_c + Y_2Y_c + Y_3Y_v$, $D = Y_cY_v$, $E = Y_2 + Y_3$, $F = Y_c + Y_v$. Here, Y_1 and Y_4 are the admittances due to the stray capacities C_1 and C_4, respectively; i.e., $J\omega C_1$ and $J\omega C_4$. Y_2 is the admittance due to C_2 and R_{sv} in parallel and Y_3 is the one due to C_3 and R_{sc} in parallel. $Y_v = 1/(R_v + R_e)$, and $Y_c = 1/(R_c + R_e)$.[2]

Z was computed from Eq. 2 by programming with complex arguments. Results of the computation revealed that at high frequencies of 1–2 kHz, the value of $|Z|$ was only slightly (3–4%) different from $|Z_{ob}|$, but at low frequency was considerably different (27% difference at 1 Hz). This is due to the fact that at low frequency Z became larger, and thus the leakage due to the sucrose columns became appreciable.

The relationship between the transfer impedance of the node and the membrane constants can be obtained from the short cable theory assuming, for the moment, that there is no end effect. The problem is to solve the transfer impedance, when a steady-state sinusoidal current is injected from one end of a short cable and the potential recorded from the other end, which is electrically open. The transfer impedance Z is given by:

$$Z = \sqrt{\frac{r_i}{y_m}} \cdot \frac{1}{\sinh(\gamma \cdot L)} \tag{3}$$

in which r_i is the internal resistance per unit length of fiber, y_m is membrane

[2] Footnote: In deriving Eq. 2 the series resistance between the nodal membrane and the ground (R_{mon} of Falk and Fatt, 1964) was neglected. The series resistance comprised the convergence resistance of the Ringer, the resistance (polarization) of the platinum black wire, and the input resistance of the I-V converter, in series, and was about 1 kΩ at 2 kHz. This is negligibly small. At this high frequency, Eq. 17 of Falk and Fatt (1964) is approximately applicable. From the equation it was estimated that under the present condition, the presence of the series resistance of 1 kΩ produced an error of less than 0.1% in the value of imaginary part of Z at 2 kHz. The error introduced to the real part is far less. At lower frequencies the error becomes less in spite of the fact that the series resistance becomes larger.

The capacity of the impedance Z_e (Fig. 2) was not included: its effect would produce a 1 or 2% error in the value of the membrane capacity.

admittance per unit length of fiber, γ is propagation constant ($= \sqrt{r_i y_m}$), and L is the nodal length. Z, y_m and γ are complex numbers. Suppose $r_i = 0$, then the decrement of the potential from one end of the fiber to the other end would vanish: this represents a condition in which the membrane properties of the node are lumped together. Under this condition:

$$Z = \frac{1}{y_m L} = \sqrt{\frac{r_i}{y_m}} \frac{1}{\gamma L}. \tag{4}$$

Assuming that at high frequency the membrane admittance y_m consists of pure capacitative element, then, the average value of γL in Table IV at 2 kHz was $\gamma L = 0.48 + J\,0.48$. Comparison of Eqs. 3 and 4 was made with this value of γL by programming with complex arguments. The computation revealed that $|Z|$ in Eq. 3 was smaller than $|Z|$ in Eq. 4 by only 0.1%, and the phase of Z in Eq. 3 lagged behind by 4°24′. At lower frequencies, the differences become smaller. Thus, under our experimental conditions, the magnitude of transfer impedance, after correcting for the capacitative and conductive leaks, can be regarded as the magnitude of membrane impedance lumped together. The high frequency capacity C_M[3] was calculated from $|Z|$ and listed in Table IV.

As shown in Table IV, the mean value of C_M is 2.86 μF/cm² at 1 kHz and 2.32 μF/cm² at 2 kHz. These values are in good agreement with the values of high frequency capacity obtained by the microelectrode technique in normal fibers (*Xenopus*, 2.61 ± 0.27 μF/cm², SEM, $n = 12$, at 2 kHz, Nakajima and Bastian, in preparation. *Rana temporaria*, 2.59 μF/cm², foot of action potential, Hodgkin and Nakajima, 1972 *b*).

The above estimation of C_M was based on an assumption that there was no end effect in the artificial node; i.e. the optically determined length of the node was assumed to represent the effective length of the node. In other words, the membrane impedance of the part inside the sucrose was assumed to be infinite. This is an approximation since some current would flow into the part of the fiber inside the sucrose through a pathway: sucrose → membrane → myoplasm. This is a system comprising one short cable (the node) flanked by two cables with very high external resistance (Jirounek and Straub, 1971). Nevertheless, the fact that the value of high frequency capacity by sucrose-gap method coincided fairly well with the value by microelectrode technique suggests that the end effect at the high frequency is not of considerable magnitude. Comparing the confidence limits (95% level) of the two sets of data, the total end effect would probably be less than 90 μm.

[3] The high frequency capacity is the magnitude of the imaginary part of the transmembrane admittance (including the input admittance of the tubular system) divided by $2\pi f$. As explained in Hodgkin and Nakajima (1972 *b*) in connection with the definition of C_f, this quantity is not a pure capacity. Nevertheless, it is a convenient quantity to compare various data.

On the other hand, at low frequency it is expected that the end effect would become substantial (Pooler and Oxford, 1972).

In conclusion, in spite of the fact that the errors due to stray capacities are small and the fact that complication from the cable property is virtually eliminated, because of the possible presence of the end-effect, the sucrose-gap method cannot be regarded as a substitute for the microelectrode technique when the main purpose is to measure the impedance accurately. Nevertheless, the measured value of capacity could be used to estimate the effective nodal length when optical means is impossible, or less reliable.

MUSCLE CONTRACTION UNDER SUCROSE-GAP One advantage of the sucrose-gap technique is that it is possible to record muscle contraction concomitant with action potential. In our method the single muscle fiber, lying at the center of the tunnel, did not touch the wall when the node contracted. Nor were there Vaseline partitions, which would have disturbed the recording of contraction. In the double sucrose-gap method, shortenings of the node were transformed into changes of tension through the long resting part of the fiber. Therefore, the recorded tension was very small, and a twitch of the node produced a force of only 80 μN (mean of 10 fibers, average diameter = 119 μm). The isometric twitch force of the fiber was about 1,700 μN (tension = 146 kN/m^2). Therefore, the node was freely shortening under an approximately constant load. (130% stretch produced a resting force of about 370 μN in the fibers). If the resting fiber, which is stretched to 130% of the resting length, could be regarded as an ideal Hookean elasticity, and the stress-strain relationship were independent of the frequency of the movement, the recorded force can easily be transformed into shortening. Actually this was not the case.

Fig. 6 illustrates the mechanical frequency response of the overall recording system, which consists of: (*a*) a resting single fiber stretched to 130%, (*b*) a glass capillary of 3-cm or 5-cm length, and (*c*) a Pixie stain-gauge, the three components being arranged as in Fig. 1. Sinusoidal stretching was applied from the free end of the fiber, and the potential output from the transducer was recorded. The sinusoidal stretch, the magnitude being about 0.7% of the slack length, was adjusted to give a tension of about the same magnitude as that generated by the twitch shortening of the node. Within this magnitude the stress-strain relation was almost linear. Therefore, we could apply a linear analysis to this system, and could recover the time-course of shortening from the recorded tension using the filter characteristic represented by Fig. 6.

Curve 1 of Fig. 7 is an example of the force of a fiber produced by a twitch of the artificial node. Curve 2 is the magnitude spectrum of Fourier transform $F(\omega)$ of curve 1 on an arbitrary linear scale. The transform was computed through the discrete Fourier transform using the fast Fourier subroutine (McGillem and Cooper, 1971). $F(\omega)$ was then divided by a vector $A(\omega)$,

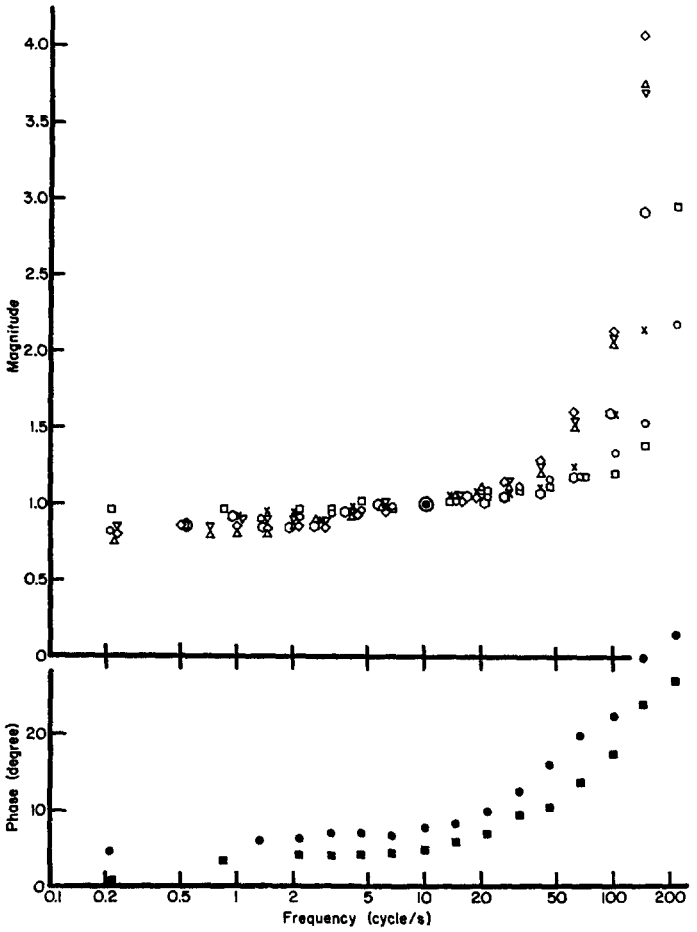

FIGURE 6. Mechanical frequency response of the recording system of contraction of the node; namely, an isolated muscle fiber (*Xenopus* flexor muscle), a glass tubing and a Pixie transducer attached in series. Experiments were done on seven isolated fibers (phase angle was measured only on two fibers). Two different glass tubings, which were used for the experiments in this series of papers, were used. This is the reason for the scatter of the data at high frequencies. Sinusoidal stretches were applied to the free end of the fiber, and the tension (output from the Pixie transducer) was analyzed in relationship with the displacement of the end of the fiber. The displacement was measured by a phototube system. Conditioning stretch of 130% of the slack length was applied. Fiber diameter ranged from 97 to 133 μm. The data were normalized to 10 Hz. Temperature 20–30°C.

which represented the mechanical frequency characteristic of resting fiber shown in Fig. 6; namely, $|F(\omega)|$ was divided by $|A(\omega)|$ and the phase of $F(\omega)$ subtracted by the phase of $A(\omega)$. The inverse transform of $F(\omega)/A(\omega)$ should represent the original shortening of the node, and this is illustrated by curve 3

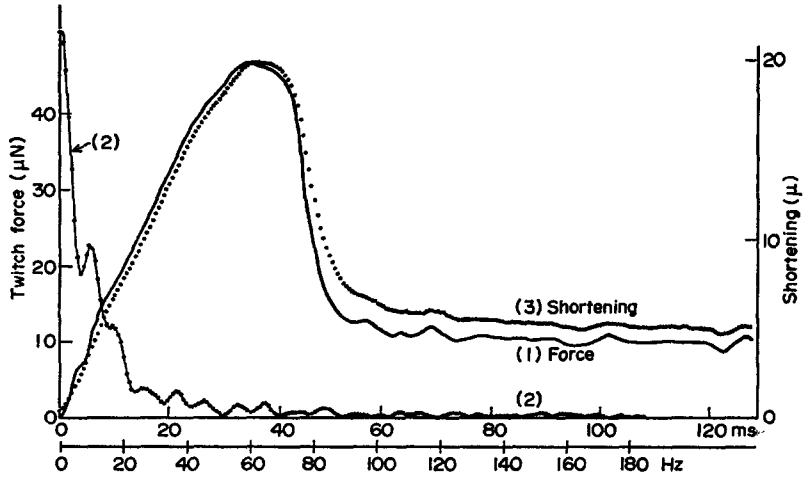

FIGURE 7. Force recorded under the sucrose gap, and the shortening curve of the node recovered by Fourier analysis. (1) An example of twitch force recorded, left-hand side ordinate. (2) $|F(\omega)|$, magnitude of Fourier transform of curve 1 on arbitrary linear scale. (3) Inverse transform of $F(\omega)/A(\omega)$, in which $A(\omega)$ is a vector representing the mechanical frequency response of the recording system shown in Fig. 6. Curve 3 should correspond to twitch shortening of the node under almost constant load. The right-hand ordinate was calculated from the average Young's module (2.23 N/mm²) of the seven fibers in Figure. 6. $|A(\omega)|$ was normalized to 5.5 Hz. The latter procedure made the height of curves 1 and 3 approximately equal. Diameter 96 μm. Nodal length 261 μm. Temperature 23.5°C.

of Fig. 7.[4] The right-hand side scale for the shortening in Fig. 7 was calculated from the average value of Young's modulus at 10 Hz obtained for the seven fibers in Fig. 6. Young's modulus which was referred to diameter at slack length and to fiber length at 130% elongation was 2.33 ± 0.45 N/mm² (Mean ± SEM n = 7) ranging from 0.78 to 4.04. Since the values of Young's modulus have great individual variations (probably due to arbitrariness in measuring the slack length), the right-hand ordinate for the shortening can hardly be regarded as precise. On the basis of this ordinate the magnitude of the shortening in Fig. 7 would be 9.9% of the slack nodal length; and the shortening speed 3.8 L/s[5] (L = slack nodal length): both values would become slightly larger if the end effect of −22 μm (see the next paper) was taken into account. For the same reason as above, these values are subject to large errors.

[4] The correctness of the program was verified by applying a wave form of muscle contraction to an *R-L* circuit. The same program recovered the original wave form very accurately from the output and the frequency response of the *R-L* circuit.

[5] In the case of frog muscle, the data of Fenn and Marsh (1935) (analyzed by Hill, 1938) indicate that the afterloaded tetanic shortening speed at 23°C is 5.6 L/s (P = 0.05 Po) and 4.6 L/s (P = 0.1 Po).

Comparison of Curves 1 and 3 of Fig. 7 indicates that although the observed force is somewhat distorted, it still represents the main feature of the original shortening of the node. In both curves, the initial constant shortening speed is set up almost immediately, the falling phase is more rapid than the rising phase, and there is a slow residual relaxation phase. These features can be seen in isotonic shortenings recorded by Jewell and Wilkie (1960) or Buchthal and Rosenfalck (1957) under different conditions. As discussed by Katz (1939), the rapid relaxation might represent a phenomenon similar to the "give" effect (Katz, 1939, page 55; Huxley and Simmons, 1970). In conclusion, the force recorded from the end of fiber can be regarded, as a first approximation, as representing isotonic shortening of the node.

DISCUSSION

The present paper has shown that although there might be differences in the mechanical properties, the electrical characteristics of normal and glycerol-treated muscles of *Xenopus* are essentially the same as those of frog. Particularly noteworthy is the finding that in the glycerol-treated muscle the value for high frequency capacity measured from the foot of action potential is near 1 $\mu F/cm^2$, in approximate agreement with the value for *Rana temporaria* (0.9 $\mu F/cm^2$, Hodgkin and Nakajima, 1972 *b*). This is an important fact for constructing an electrical model of muscle membrane involving both surface and transverse tubular membranes (Falk and Fatt, 1964; Adrian et al., 1969; Schneider, 1970; Gage and Eisenberg, 1969; Valdiosera et al., 1974). The fact is also interesting in that it indicates the general similarity of membrane characteristics among various kinds of biological membranes (Cole, 1968).

One advantage of using *Xenopus* is that it is relatively easy to apply the sucrose-gap method to single muscle fibers. With the sucrose gap it is possible to record mechanical events concomitant with the electrical phenomena of a small area of the muscle fiber (cf. Adrian et al., 1970; Moore, 1972). Although a strict comparison is impossible because of the differences in the sampling procedures, the action potential of *Xenopus* muscle recorded with the sucrose-gap method does not seem to be much different from that recorded with the intracellular electrode, except for the hyperpolarization and a slight tendency toward slowing down of the repolarization phase.

However, as examined in detail in this paper there are several technical problems inherent to this method. One problem is the stray capacities, and this would have introduced errors in measuring high frequency events unless they are minimized by proper construction and shielding of the apparatus. Another is the uncertainty in estimating the nodal length, even with the absence of Vaseline partitions, due to the presence of the end effect. Finally, muscular contraction recorded from one end of the fiber is distorted by the viscoelastic property of resting fiber. Fortunately, under the present experi-

mental conditions the recorded force could be regarded approximately as isotonic shortening of the node. Similar analyses could probably be applicable to the "tension" of the heart muscles recorded with the sucrose-gap method (Beeler and Reuter, 1970; Morad and Orkand, 1971; New and Trautwein, 1972; Vassort and Rougier, 1972). The analyses described in the present paper indicate that proper allowances should always be made for these complications when drawing a conclusion from experiments using this method. The next paper (Bastian and Nakajima, 1974) demonstrates the application of the sucrose gap in elucidating a problem concerning the muscle activation.

We wish to thank Dr. Makoto Endo for his advice throughout the investigation. We thank him and Dr. R. S. Eisenberg for critically reading the manuscript and giving valuable suggestions, and Dr. G. W. Hughes for advice concerning computer programming.

We are also indebted to Drs. M. Ildefonse, J. W. Moore, T. Narahashi, and O. Rougier for helpful suggestions about the sucrose gap technique.

The work was supported by PHS Grant NS-08601 and PHS Training Grant NS-2380.

Received for publication 27 July 1973.

REFERENCES

ADRIAN, R. H., W. K. CHANDLER, and A. L. HODGKIN. 1969. The kinetics of mechanical activation in frog muscle. *J. Physiol. (Lond.).* **204**:207.

ADRIAN, R. H., W. K. CHANDLER, and A. L. HODGKIN. 1970. Voltage clamp experiments in striated muscle fibres. *J. Physiol. (Lond.).* **208**:607.

BASTIAN, J., and S. NAKAJIMA. 1974. Action potential in the transverse tubules and its role in the activation of skeletal muscle. *J. Gen. Physiol.* **63**:257.

BEELER, G. W., JR., and H. REUTER. 1970. The relation between membrane potential, membrane currents and activation of contraction in ventricular myocardial fibres. *J. Physiol. (Lond.).* **207**:211.

BLAUSTEIN, M. P., and D. E. GOLDMAN. 1966. Origin of axon membrane hyperpolarization under sucrose-gap. *Biophys. J.* **6**:453.

BUCHTHAL, F., and P. ROSENFALCK. 1957. Elastic properties of striated muscle in "Tissue Elasticity." J. W. Remington, editor. Waverly Press Inc., Baltimore. 73.

CHAPMAN, R. A. 1970. High sensitivity isometric force transducers made with piezo-electric or piezo-resistive strain gauges. *J. Physiol. (Lond.).* **210**:4*P*.

COLE, K. S. 1968. Membranes, Ions and Impulses. University of California Press, Berkeley, Calif.

FALK, G., and P. FATT. 1964. Linear electrical properties of striated muscle fibers observed with intracellular electrodes. *Proc. R. Soc. Lond. B Biol. Sci.* **160**:69.

FENN, W. O., and B. S. MARSH. 1935. Muscular force at different speeds of shortening. *J. Physiol. (Lond.).* **85**:277.

GAGE, P. W., and R. S. EISENBERG. 1969. Capacitance of the surface and transverse tubular membrane of frog sartorius muscle fibers. *J. Gen. Physiol.* **53**:265.

HILL, A. V. 1938. The heat of shortening and the dynamic constants of muscle. *Proc. R. Soc. Lond. B Biol. Sci.* **126**:136.

HODGKIN, A. L., and S. NAKAJIMA. 1972 *a*. The effect of diameter on the electrical constants of frog's skeletal muscle fibers. *J. Physiol. (Lond.).* **221**:105.

HODGKIN, A. L., and S. NAKAJIMA. 1972 *b*. Analysis of the membrane capacity in frog muscle. *J. Physiol. (Lond.).* **221**:121.

HOWELL, J. N., and D. J. JENDEN. 1967. T-tubules of skeletal muscle; morphological alterations which interrupt excitation-contraction coupling. *Fed. Proc.* **26**:553.

HUXLEY, A. F., and R. M. SIMMONS. 1970. Rapid "give" and the tension "shoulder" in the relaxation of frog muscle fibers. *J. Physiol. (Lond.).* **210**:32*P*.

ILDEFONSE, M., and O. ROUGIER. 1972. Voltage-clamp analysis of the early current in frog skeletal muscle fibre using the double sucrose-gap method. *J. Physiol. (Lond.)*. **222**:373.

JEWELL, B. R., and D. R. WILKIE. 1960. The mechanical properties of relaxing muscle. *J. Physiol. (Lond.)*. **152**:30.

JIROUNEK, P., and R. W. STRAUB. 1971. The potential distribution and the short-circuiting factor in the sucrose-gap. *Biophys. J.* **11**:1.

JULIAN, F. J., J. W. MOORE, and D. E. GOLDMAN. 1962. Membrane potentials of the lobster giant axon obtained by use of the sucrose-gap technique. *J. Gen. Physiol.* **45**:1195.

KATZ, B. 1939. The relation between force and speed in muscular contraction. *J. Physiol. (Lond.)*. **96**:45.

KROLENKO, S. A. 1969. Changes in the T-system of muscle fibres under the influence of influx and efflux of glycerol. *Nature (Lond.)*. **221**:966.

KROLENKO, S. A., and V. V. FEDOROV. 1972. Recovery of isometric twitches after glycerol removal. *Experientia (Basel)*. **28**:424.

MOORE, L. E. 1972. Voltage clamp experiments on single muscle fibers of *Rana pipiens*. *J. Gen. Physiol.* **60**:1.

MORAD, M., and R. K. ORKAND. 1971. Excitation-contraction coupling in frog ventricle: evidence from voltage clamp studies. *J. Physiol. (Lond.)*. **219**:167.

MCGILLEM, C. D., and G. R. COOPER. 1971. Continuous and discrete signal and system analysis. Holt, Rinehart and Winston, Inc., New York.

NAKAJIMA, S., Y. NAKAJIMA, and L. D. PEACHEY. 1973. Speed of repolarization and morphology of glycerol-treated frog muscle fibers. *J. Physiol. (Lond.)*. **234**:465.

NEW, W., and W. TRAUTWEIN. 1972. The ionic nature of slow inward current and its relation to contraction. *Pfluegers Arch. Eur. J. Physiol.* **334**:24.

POOLER, J. P., and G. S. OXFORD. 1972. Low membrane resistance in sucrose-gap—a parallel leakage path. *Biochim. Biophys. Acta.* **255**:681.

SCHNEIDER, M. F. 1970. Linear electrical properties of the transverse tubules and surface membrane of skeletal muscle fibers. *J. Gen. Physiol.* **56**:640.

STÄMPFLI, R. 1963. Die doppelte Saccharosetrennwandmethode zur Messung von elektrischen Membraneigenschaften mit extracellularen Elektroden. *Helv. Physiol. Pharmacol. Acta.* **21**:189.

VALDIOSERA, R., C. CLAUSEN, and R. S. EISENBERG. 1974. The impedance of frog skeletal muscle fibers in various solutions. In press.

VASSORT, G., and O. ROUGIER. 1972. Membrane potential and slow inward current dependence of frog cardiac mechanical activity. *Pfluegers Arch. Eur. J. Physiol.* **331**:191.

ZACHAR, J., D. ZACHAROVA, and R. H. ADRIAN. 1972. Observations on "detubulated" muscle fibres. *Nat. New Biol.* **239**:153.